12 A brief review of other methods of computer simulation

12.1 INTRODUCTION

In the previous chapters of this text we have examined a wide variety of Monte Carlo methods in depth. Although these are exceedingly useful for many different problems in statistical physics, there are some circumstances in which the systems of interest are not well suited to Monte Carlo study. Indeed there are some problems which may not be treatable by stochastic methods at all, since the time-dependent properties as constrained by deterministic equations of motion are the subject of the study. The purpose of this chapter is thus to provide a very brief overview of some of the other important simulation techniques in statistical physics. Our goal is not to present a complete list of other methods or even a thorough discussion of these methods which are included, but rather to offer sufficient background to enable the reader to compare some of the different approaches and better understand the strengths and limitations of Monte Carlo simulations.

12.2 MOLECULAR DYNAMICS

12.2.1 Integration methods (microcanonical ensemble)

Molecular dynamics methods are those techniques which are used to numerically integrate coupled equations of motion for a system which may be derived, e.g. in the simplest case from Lagrange's equations or Hamilton's equations. Thus, the approach chosen is to deal with many interacting atoms or molecules within the framework of classical mechanics. We begin this discussion with consideration of systems in which the number of particles N, the system volume V, and the total energy of the system E are held constant. This is known as the NVE ensemble. In the first approach, Lagrange's equations for N particles produce a set of $3N$ equations to be solved:

$$m_i \ddot{\mathbf{r}}_i = \mathbf{F}_i = -\nabla_{r_i} v, \tag{12.1}$$

where m_i is the particle mass and $\mathbf{F}_\mathrm{i}$ the total net force acting on each particle (v is the appropriate potential). For N particles in three spatial dimensions ($d = 3$) this entails the solution of $3N$ second order equations. (The reader

will recognize Eqn. (12.1) as Newton's second law.) If instead, Hamilton's equations are used to derive the system dynamics, a set of $6N$ first order equations will result:

$$\dot{\mathbf{r}}_i = \mathbf{p}_i / m_i, \tag{12.2a}$$

$$\dot{\mathbf{p}}_i = \mathbf{F}_i. \tag{12.2b}$$

where $\mathbf{p}_i$ is the momentum of the particle. Either set of equations can be solved by simple finite difference methods using a time interval Δ, which must be made sufficiently small to maintain accuracy. It is clear from the Hamilton's equation approach that the energy of the system is invariant with time so that solution of these equations produces states in the microcanonical ensemble. The simplest numerical solution is obtained by making a Taylor expansion of the position and velocity about the current time t, i.e.

$$\mathbf{r}_i(t + \Delta) = \mathbf{r}_i(t) + \mathbf{v}_i(t)\Delta + \frac{1}{2}\mathbf{a}_i(t)\Delta^2 + \cdots, \tag{12.3a}$$

$$\mathbf{v}_i(t + \Delta) = \mathbf{v}_i(t) + \mathbf{a}_i(t)\Delta + \cdots. \tag{12.3b}$$

These equations are truncated after a small number of terms so that the calculation of the properties of each particle at the next time is straightforward, but errors tend to build up rather quickly after many time steps have passed. In order to minimize truncation errors two-step predictor–corrector methods may be implemented. In these approaches a prediction is made for the new positions, velocities, etc., using the current and previous values of these quantities, and then the predicted acceleration is used to calculate improved (or corrected) positions, velocities, etc. A number of different predictor-corrector methods have been considered and the comparison has been made elsewhere, see e.g. Berendsen and van Gunsteren (1986).

No discussion of molecular dynamics methods, not even an introductory one, would be complete without some presentation of the Verlet algorithm (Verlet, 1967). The position $\mathbf{r}_i$ is expanded using increments $+\Delta$ and $-\Delta$ and the resultant equations are then added to yield

$$\mathbf{r}_i(t + \Delta) = \mathbf{r}_i(t) - \mathbf{r}_i(t - \Delta) + \mathbf{a}_i(t)\Delta^2 + \ldots. \tag{12.4}$$

The velocities are then determined by taking numerical time derivatives of the position coordinates

$$\mathbf{v}_i(t) = \frac{\mathbf{r}_i(t + \Delta) - \mathbf{r}_i(t - \Delta)}{2\Delta}. \tag{12.5}$$

Note that the error in Eqn. (12.4) has been reduced to order Δ^4 but the error in the velocity is of order Δ^2. There are a number of other schemes for carrying out the integration over time that have been developed and these are discussed by Allen and Tildesley (1987) and Rapaport (1995). Molecular dynamics studies have played an extremely important role in the development of computer simulations, and indeed the discovery of long time tails (algebraic decay) of the velocity autocorrelation function in a simple hard sphere model

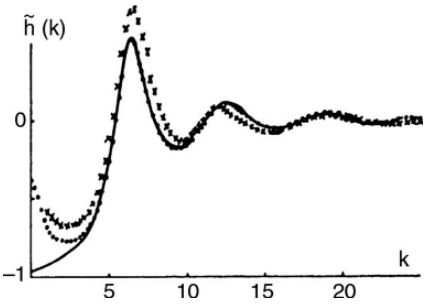

Fig. 12.1 Pair correlation function $\tilde{h}(k)$ for a classical fluid: (dots) molecular dynamics data for a Lennard–Jones potential with $T = 1.326$, $\rho = 0.5426$; (solid curve) hard-sphere model; (crosses) x-ray experiment on argon. From Verlet (1968).

was a seminal work that provided important insights into liquid behavior (Alder and Wainwright, 1970).

In these microcanonical simulations both the kinetic energy and the potential energy will vary, but in such a way as to keep the total energy fixed. Since the temperature is proportional to the mean kinetic energy, i.e.

$$\frac{1}{2}\sum_i m_i \dot{r}_i^2 = \frac{3}{2} N k_B T, \tag{12.6}$$

it will fluctuate during the course of the simulation on a finite system. Similarly, the potential energy will vary as the particles move, but these variations can be determined by direct measurement. Obviously the use of such techniques for obtaining averages in thermal equilibrium relies on the ergodicity property of the system. Typical time steps are in the sub-picosecond range and molecular dynamics simulations can generally follow a system for only tens or hundreds of nanoseconds. Therefore, it is only possible to study problems where equilibrium is reached on such a short time scale. Characteristic of the kinds of studies that can be performed using molecular dynamics are investigations of classical fluid models in which the particles interact via a Lennard–Jones potential (see Eqn. (6.4)). Figure 12.1 shows the equilibrium correlations obtained for a dense fluid of 864 particles (Verlet, 1968).

More recently there have been improvements made in the use of higher order decompositions, which are based on the Trotter formula, for the integration of coupled equations of motion which describe different kinds of motions with very different time scales (Tuckerman *et al.*, 1992). In this approach the 'slow' degrees of freedom are frozen while the others are updated using a rather fine time scale; the 'slow' degrees of freedom are then updated using a coarse time scale.

Some time integration methods are better at conserving energy, or other 'constants of the motion' while some methods are capable of determining other physical properties with greater accuracy or speed even though the exact preservation of conservation properties is lost. One important consideration is the conservation of phase space volume. Only integration methods which have

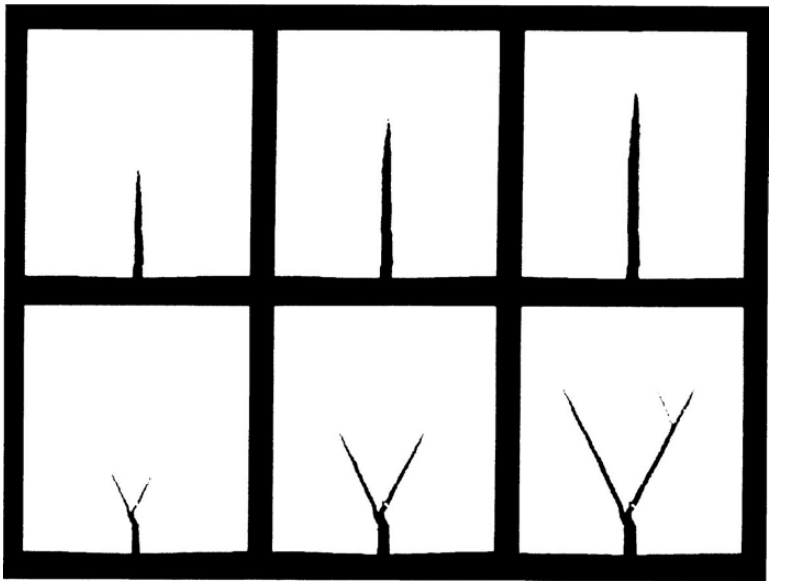

Fig. 12.2 Results of a molecular dynamics study of the time evolution of crack propagation in a model with modified Lennard–Jones interactions. The top row shows time sequences for initial motion in the stiff direction, and in the bottom row the initial motion is in the soft direction. From Abraham (1996).

time reversal symmetry will conserve a given volume in phase space, and algorithms which are time reversible generally have less long term drift of conserved quantities than those which are not time reversal invariant. Molecular dynamics methods have been well suited to vectorization and, more recently, efficient parallel algorithms have been constructed that allow the study of quite large systems. For example, in Fig. 12.2 we show some results of fracture in a system of about 2×10^6 particles interacting with a modified Lennard–Jones potential. We emphasize that such a large number of particles by no means is the 'world record' for size. As far back as 2000, Roth *et al.* (2000) ran some 5 billion atoms on a CRAY T3E using 512 processors, albeit only for five integration time steps. More recently, more than 19 billion particles were run for 50 MD time steps on the QSC machine of Los Alamos (Kadau *et al.*, 2004), also demonstrating the very good scalability properties of the SPaSM code (Beazley and Lomdahl, 1994) that was used. For such large problems, the analysis of configurations needs to be done 'on the fly', due to the large number of coordinates and momenta that need to be handled; and, furthermore, the use of visualization tools presents special problems. It is clear that such feasibility studies have not yet produced useful results on physics problems, but they do demonstrate the prospect that, in a few years, materials science problems on the μm scale may become accessible to direct atomistic simulation. Historically, the choice of algorithm was often determined in large part by the amount of computer memory needed, i.e. the number of variables that needed to be kept track of. Given the large memories available today, this concern has been largely ameliorated. Two features that we do want to mention here, which were introduced to make molecular dynamics simulations faster, are potential 'cutoffs' and 'neighbor lists'. (These labor saving devices can also be used for Monte Carlo simulations of systems with continuous symmetry.)

As the particles move, the forces acting on them change and need to be continuously recomputed. A way to speed up the calculation with only a modest reduction in accuracy is to cut off the interaction at some suitable range and then make a list of all neighbors which are within some slightly larger radius. As time progresses, only the forces caused by neighbors within the 'cutoff radius' need to be recomputed, and for large systems the reduction in effort can be substantial. (The list includes neighbors which are initially beyond the cutoff but which are near enough that they might enter the 'interacting region' within the number of time steps, typically 10–20, which elapse before the list is updated.) With the advent of parallel computers, molecular dynamics algorithms have been devised that will distribute the system over multiple processors and allow treatment of quite large numbers of particles. One major constraint which remains is the limitation in maximum integration time and algorithmic improvement in this area is an important challenge for the future. There are a number of important details and we refer the reader elsewhere (Allen and Tildesley, 1987; Rapaport, 1995) for the entire story.

Problem 12.1 Consider a cubic box of fixed volume V and containing $N = 256$ particles which interact with a Lennard–Jones potential suitable for argon: $\sigma = 0.3405$ nm, $\epsilon/k_B = 119.8$ K, $m = 6.63382 \times 10^{-26}$ kg ($T^* = k_B T/\varepsilon$, $\rho^* = \rho\sigma^3$). Use a simple Verlet algorithm with a cutoff of $r = 2.5\sigma$ to carry out a molecular dynamics simulation with a density of $\rho^* = 0.636$ and a total (reduced) energy E^* of 101.79. Please answer the following questions:

(a) What is the average temperature T^* for the system?
(b) What is the time dependence of the kinetic energy for the system?
(c) What is the time dependence of the potential energy for the system?

12.2.2 Other ensembles (constant temperature, constant pressure, etc.)

Often the properties of the system being studied are desired for a different set of constraints. For example, it is often preferable to have information at constant temperature rather than at constant energy. This can be accomplished in several different ways. The crudest approach is simply to periodically rescale all of the velocities so that the total kinetic energy of the systems remains constant. This basic approach can also be implemented in a stochastic manner in which the velocity of a randomly chosen particle is reset using a Maxwell–Boltzmann distribution. A very popular method is that of 'thermostats' in which an additional degree of freedom is added to play the role of a reservoir (Nosé, 1984; Hoover, 1985). The time integration is then carried out for this extended system and energy is extracted from the reservoir or inputted to it from the system so as to maintain a constant system temperature. The equations of motion which must then be solved are different from the original expressions; if we denote the particle position by $\mathbf{r}$ and the 'new' degree of

freedom by s, the equations to be solved for a particle of mass m become

$$\ddot{\mathbf{r}}_i = \mathbf{F}_i/m_i s^2 - 2\dot{s}\dot{\mathbf{r}}_i/s, \tag{12.7a}$$

$$Q\ddot{s} = \sum_i m_i \dot{r}_i^2 s - (f+1)k_B T/s, \tag{12.7b}$$

where f is the number of degrees of freedom, T is the desired temperature, and Q represents the size of the 'thermal ballast'. There will, of course, be some thermal lag and/or overshoot if this process is not carried out carefully, i.e. if Q is not chosen wisely, but when care is exercised the net result is usually quite good.

Molecular dynamics simulations can also be carried at constant pressure using several different techniques including 'barostat' methods, which are the equivalent of the thermostats described above (Andersen, 1980). Constant pressure may also be maintained by changing the box size, and more sophisticated algorithms even allow for a change in the shape of the simulation box. This latter capability may be important for the study of solids that exhibit structural phase changes which may be masked or inhibited by a fixed shape for the simulation box. Obviously it is possible to include both thermostats and barostats to work in the NpT ensemble.

A rather different approach to molecular dynamics may be taken by considering a system of perfectly 'hard' particles which only interact when they actually collide. The purpose of this simplification is to enable rather large numbers of particles in relatively low density systems to be simulated with relatively modest resources. For studies of hard particles the algorithms must be modified rather substantially. The (straight line) trajectories of each of the particles are calculated and the time and location of the next collision are determined. The new velocities of the colliding particles are calculated using conservation of energy and momentum for elastic collisions and the process is resumed. Thus, instead of being a time-step-driven process, hard particle molecular dynamics becomes an event-driven method. Such simulations have been quite successful in producing macroscopic phenomena such as the Rayleigh–Bénard instability, shown in Fig. 12.3, in a two-dimensional system (Rapaport, 1988) confined between two horizontal plates held at different temperatures. The data show that the formation of the final, steady-state roll pattern takes quite some time to develop.

Problem 12.2 Take the system which you used in Problem 12.1 and carry out a constant temperature MD simulation at the temperature which you found from Problem 12.1. Determine:

- **(a)** the average kinetic energy for the system;
- **(b)** the average potential energy for the system;
- **(c)** the average total energy for the system. Compare with the value of E^* in Problem 12.1.

In the example shown in Fig. 12.1 we have used the pair correlation function, i.e. a static quantity in thermal equilibrium, which could have been evaluated

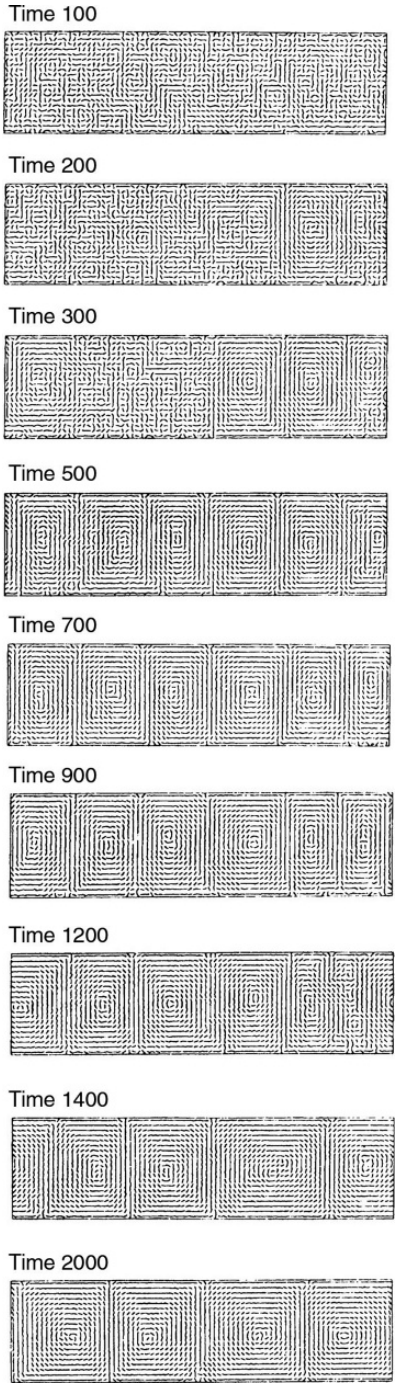

Fig. 12.3 Development of coarse-grained flow lines for the Rayleigh–Bénard instability as determined from hard particle molecular dynamics simulations. From Rapaport (1988).

with Monte Carlo methods as well (see Chapter 6). In fact, molecular dynamics often is used to address static equilibrium properties only, ignoring the additional bonus that dynamical properties could be obtained as well. This approach makes sense in cases where molecular dynamics actually produces statistically independent equilibrium configurations faster than corresponding Monte Carlo simulations. Such situations have been reported, e.g. in the simulation of molten SiO_2 (due to strong covalent bonds Monte Carlo moves where the random movement of single atoms to new positions has a low acceptance rate), models of polymer melts near their glass transition, etc. For problems of this type, the decision whether Monte Carlo or molecular dynamics algorithms should be used is non-trivial, because the judgment of efficiency is subtle. Sometimes Monte Carlo is superior due to non-local moves, such as pivot rotations of large parts of long polymer chains (see Chapter 6).

12.2.3 Non-equilibrium molecular dynamics

In the entire discussion given above, the goal was to produce and study the behavior of an interacting system of particles in equilibrium. For systems which are not in equilibrium, e.g. systems subject to a large perturbation, the techniques used must be altered. In methods of non-equilibrium molecular dynamics a large perturbation is introduced and transport coefficients are then measured directly. Either the perturbation may be applied at time $t = 0$ and the correlation functions are measured and integrated to give transport coefficients, or an oscillating perturbation is applied and the real and imaginary responses are measured by Laplace transform of the correlation functions.

There is now a large body of work focused on the study of fluids under steady-state shear (for early reviews of the simulation technique, see Evans and Morriss (1984, 1990)). Steady-state shear creates specific problems due to the dissipated heat that the thermostat needs to remove to avoid having the system heat up (Pastorino *et al.*, 2007). This steady-state shear can be realized either by the Lees–Edwards 'sliding brick' boundary conditions or by movement of real walls in opposite directions.

12.2.4 Hybrid methods (MD + MC)

For some complex systems Monte Carlo simulations have very low acceptance rates except for very small trial moves and hence become quite inefficient. Molecular dynamics simulations may not allow the system to develop sufficiently in time to be useful, however, molecular dynamics methods may actually improve a Monte Carlo investigation of the system. A trial move is produced by allowing the molecular dynamics equations of motion to progress the system through a rather large time step. Although such a development may no longer be accurate as a molecular dynamics step, it will produce a Monte Carlo trial move which will have a much higher chance of success than

a randomly chosen trial move. In the actual implementation of this method some testing is generally advisable to determine an effective value of the time step (Duane *et al.*, 1987).

One example of the utility of this technique was given by Tavazza *et al.* (2004) who used a hybrid MC-MD algorithm for the study of islands and step edges on semiconductor surfaces. Because of the dimerization that occurs at Si surfaces, the diffusion of adatoms is accompanied by significant reconstruction and local energy changes. One consequence of this behavior is that standard single particle Monte Carlo moves are virtually never accepted. But by adapting the hybrid MC-MD algorithm to the movement of an adatom and its initial and final environments, thermal fluctuations of islands of adatoms could be investigated.

12.2.5 *Ab initio* molecular dynamics

No discussion of molecular dynamics would be complete without at least a brief mention of the approach pioneered by Car and Parrinello (1985), which combines electronic structure methods with classical molecular dynamics. In this hybrid scheme a fictitious dynamical system is simulated in which the potential energy is a functional of both electronic and ionic degrees of freedom. This energy functional is minimized with respect to the electronic degrees of freedom to obtain the Born–Oppenheimer potential energy surface to be used in solving for the trajectories of the nuclei. This approach has proven to be quite fruitful with the use of density functional theory for the solution of the electronic structure part of the problem and appropriately chosen pseudopotentials.

The Lagrangian for the system is

$$L = 2\sum_i \int d\mathbf{r}\mu_i |\dot{\psi}_i(\mathbf{r})|^2 + \frac{1}{2}\sum_I M_I \dot{R}_I^2 - E\left[\{\psi_a\}\mathbf{R}_I\right] + 2\sum_{ij}\Lambda_{ij}\left(\int d\mathbf{r}\psi_i^*(\mathbf{r})\psi_j(\mathbf{r}) - \delta_{ij}\right), \tag{12.8}$$

where E is the energy functional, ψ_i the single particle wave function, M_I and R_I the ionic masses and positions respectively. μ_i is the fictitious electronic mass and the fictitious dynamics is given by

$$\dot{\psi}_\mathrm{i}(\mathbf{r}, t) = -\frac{1}{2}\frac{\delta E}{\delta \psi_i^*(\mathbf{r}, t)}. \tag{12.9}$$

(Note that the single particle wave functions play the role of fictitious classical dynamic variables.) The Λ_{ij} are Lagrangian multipliers that are used to maintain the orthonormality of the single particle wave functions. The resultant

equations of motion are

$$\mu_i \ddot{\psi}_i(\mathbf{r}, t) = -\frac{1}{2}\frac{\delta E}{\delta \psi_i^*(\mathbf{r}, t)} + \sum_j \Lambda_{ij}\psi_j(\mathbf{r}, t), \tag{12.10a}$$

$$M_I \ddot{\mathbf{R}}_I = -\frac{\partial E}{\partial \ddot{\mathbf{R}}_I(t)}. \tag{12.10b}$$

These equations of motion can then be solved by the usual numerical methods, e.g. the Verlet algorithm, and constant temperature simulations can be performed by introducing thermostats or velocity rescaling. This *ab initio* method is efficient in exploring complicated energy landscapes in which both the ionic positions and electronic structure are determined simultaneously (Parrinello, 1997).

12.2.6 Hyperdynamics and metadynamics

For many systems molecular dynamics trajectories can be largely described by a series of very infrequent 'transitions' from one potential minimum to another. In such cases, traversing the path from one basin to another with molecular dynamics may not only take a great deal of CPU time, but also the potential surface through which they pass may change with time. Voter (1997) introduced the concept of 'hyperdynamics' to accelerate the process. He introduced a bias potential (ΔV) that raises the energy in regions that are outside the transition states between potential minima. One important feature of this approach is that it does not require advance knowledge of the actual potential surface yet can accelerate molecular dynamics simulations by orders of magnitude.

A related approach is that of 'metadynamics' (Laio and Parrinello, 2002, 2006). First, a set of collective variables $\{s\}$ is identified, and the dynamics of these variables is then driven by the free energy, which is biased by a history dependent potential $F_G(s, t)$ constructed as a sum of Gaussians centered along the previous trajectory followed by the collective variables. (This methodology can be viewed as a finite temperature extension of Wang–Landau sampling (Laio and Parrinello, 2006).) If properly constructed, the potential $F_G(s, t)$ provides an unbiased estimate of the free energy of the system, and the effective potential energy surface for the time dependence becomes rather flat, thus allowing the system to move easily from one energy basin to another. Combined with Car–Parrinello molecular dynamics, this approach has proven to be effective for complicated chemical processes.

12.3 QUASI-CLASSICAL SPIN DYNAMICS

Although the static properties of a large number of magnetic systems have been well studied experimentally, theoretically, and via simulation, the study of the dynamic properties of magnetic systems is far less mature. The Monte

Carlo method is fundamentally stochastic in nature and in general there is no correlation between the development of a system in Monte Carlo time and in real time, although the static averages are the same (by construction). An approach to the investigation of true time-dependent properties is to generate initial states, drawn from a canonical ensemble using Monte Carlo methods, and to use these as starting points for the integration of the coupled equations of motion. For example, consider a system of N spins which interact with the general Hamiltonian

$$\mathcal{H} = -\mathcal{J} \sum_{\langle i,j \rangle} \left(S_{ix} S_{jx} + S_{iy} S_{jy} + \lambda S_{iz} S_{jz} \right) + D \sum_i S_{iz}^2 - H \sum_i S_{iz}, \tag{12.11}$$

where the first sum is over all nearest neighbor pairs, λ represents exchange anisotropy, D is the single ion anisotropy, and H is the external magnetic field. There are a number of physical systems which are well approximated by Eqn. (12.11), although for different systems one or more of the parameters may vanish. For $\lambda = 1$ and $D = 0$ this represents the isotropic Heisenberg ferromagnet or the corresponding antiferromagnet for $\mathcal{J} > 0$ or $\mathcal{J} < 0$, respectively.

For models with continuous degrees of freedom, real equations of motion can be derived from the quantum mechanical commutator,

$$\frac{\partial \hat{\mathbf{S}}_i}{\partial t} = -\frac{i}{\hbar} [\hat{\mathbf{S}}_i, \ \mathcal{H}], \tag{12.12a}$$

by allowing the spin value to go to infinity and normalizing the length to unity to yield

$$\frac{d\mathbf{S}_i}{dt} = \frac{\partial \mathcal{H}}{\partial \mathbf{S}_i} \times \mathbf{S}_i = -\mathbf{S}_i \times \mathbf{H}_{\text{eff}}, \tag{12.12b}$$

where $\mathbf{H}_{\text{eff}}$ is an 'effective' interaction field. For the isotropic Heisenberg ferromagnet $\mathbf{H}_{\text{eff}} = -\mathcal{J} \sum_{nn} \mathbf{S}_j$, and the time dependence of each spin, $\mathbf{S}_{\text{r}}(t)$, can be determined from integration of these equations. These coupled equations of motion can be viewed as describing the precession of each spin about an effective interaction field; the complexity arises from the fact that since all spins are moving, the effective field is not static but rather itself constantly changing direction and magnitude.

A number of algorithms are available for the integrations of the coupled equations of motion which were derived in the previous sub-section. The simplest approach is to expand about the current spin value using the time step Δ as the expansion variable:

$$S_i^\alpha (t + \Delta) = S_i^\alpha (t) + \Delta \dot{S}_i^\alpha (t) + \frac{1}{2} \Delta^2 \ddot{S}_i^\alpha (t) + \frac{1}{3!} \Delta^3 \dddot{S}_i^\alpha (t) + \cdots, \tag{12.13}$$

where the α denotes the spin component. (Compare this equation with Eqn. (12.3) for molecular dynamics.) The 'new' estimate may be made by simply evaluating as many terms as possible in the sum, although this

procedure must obviously be truncated at some point. Typical values of Δ which deliver reliable results to a reasonable maximum integration time $t_{\max}$ are in the range of $\Delta = 0.005$. If the equation is truncated at the point shown in Eqn. (12.13), the errors will be of order Δ^4. A very simple improvement can be made by implementing a 'leapfrog' procedure (in the spirit of Eqn. (12.4)) to yield (Gerling and Landau, 1984)

$$S_i^\alpha(t+\Delta) = S_i^\alpha(t-\Delta) + 2\Delta\dot{S}_i^\alpha(t) + \frac{2}{3!}\Delta^3\dddot{S}_i^\alpha(t) + \cdots. \quad (12.14)$$

The error in this integration is $O(\Delta^5)$ and allows not only larger values of Δ to be used but also allows us to extend the maximum integration time to $t_{\max} \approx 100\mathcal{J}^{-1}$. Several standard numerical methods can also be applied. One excellent approach is to use a predictor–corrector method; fourth order predictor–corrector methods have proven to be quite effective for spin dynamics simulations. An example is the explicit four-step Adams–Bashforth method (Burden *et al.*, 1981) followed by an implicit Adams–Moulton corrector step, a combination which also has a local truncation error of Δ^5 and which has proven to be quite successful. The first application of this method requires that at least three time steps have already been taken; these can initially be provided using the fourth order Runge–Kutta method, starting with the initial state. Of course, this predictor–corrector method requires that the spin configuration at four time steps must be kept in memory. Note that the conservation laws discussed earlier will only be observed within the accuracy set by the truncation error of the method. In practice, this limits the time step to typically $\Delta = 0.01\mathcal{J}^{-1}$ in $d = 3$ (Chen and Landau, 1994) for the isotropic model ($D = 0$), where $t_{\max} \leq 200\mathcal{J}^{-1}$. The same method was used in $d = 2$; with $\Delta = 0.01\mathcal{J}^{-1}$, $t_{\max} = 400\mathcal{J}^{-1}$ (Evertz and Landau, 1996) could be achieved, and this was sufficient to provide an excellent description of the dynamic structure factor for the two-dimensional XY-model at the Kosterlitz–Thouless transition as shown in Fig. 12.4. This result presents a real theoretical challenge, since none of the existing theoretical predictions (labeled NF (Nelson and Fisher, 1977) and Villain (1974) in the figure) can explain either the central peak or the shape of the spin wave peak. Note that the high frequency intensity falls off as a power law, in agreement with the NF theory.

For a typical spin dynamics study the major part of the CPU time needed is consumed by the numerical time integration. The biggest possible time step is thus most desirable, however, 'standard' methods impose a severe restriction on the size of Δ for which the conservation laws of the dynamics are obeyed. It is evident from Eqn. (12.11) that $|\mathrm{S}_i|$ for each lattice site i and the total energy are conserved. Symmetries of the Hamiltonian impose additional conservation laws, so, for example, for $D = 0$ and $\lambda = 1$ (isotropic Heisenberg model) the magnetization $\mathbf{m}$ is conserved. For an anisotropic Heisenberg model, i.e. $\lambda \neq 1$ or $D \neq 0$, only the z-component m_z of the magnetization is conserved. Conservation of spin length and energy is particularly crucial, and it would therefore also be desirable to devise an algorithm which conserves these two quantities exactly. In this spirit, a new, large time step integration procedure,

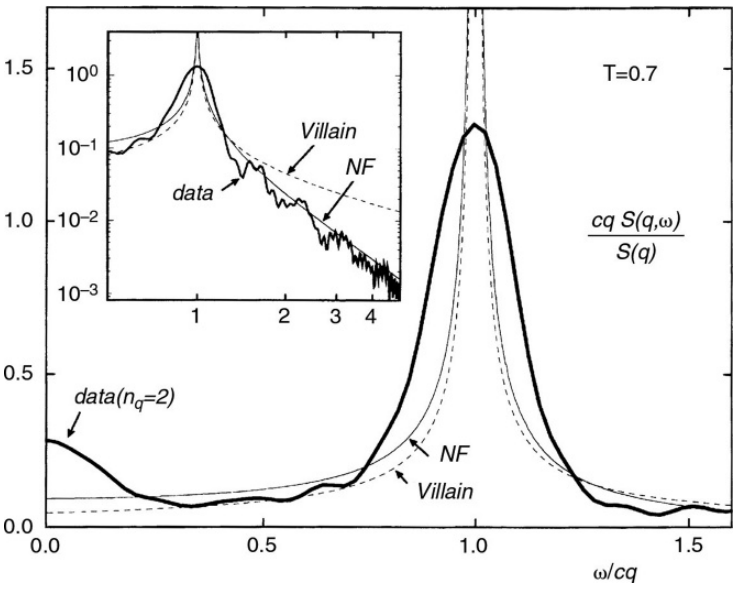

Fig. 12.4 Dynamic structure factor for the two-dimensional XY-model at T_{KT}. The heavy curve shows data obtained from spin dynamics simulations, and the light lines are theoretical predictions. From Evertz and Landau (1996).

which is based on Trotter–Suzuki decompositions of exponential operators and conserves both spin length and energy *exactly* for $D = 0$, has been devised (Krech *et al.*, 1998). Variants of this method for more general models allow very large time steps but do not necessarily conserve all quantities exactly. The conservation is nonetheless good enough for practical application. These decomposition spin dynamics methods have been used to study the simple cubic Heisenberg antiferromagnet, a model that is a very good representation of the physical system $RbMnF_3$. Disagreements between experiment and theory for the dynamic critical exponent have existed since the 1970s for this system. The structure factor determined from simulation was compared with new experimental data and quantitative agreement was quite good at several temperatures (Tsai *et al.*, 2000). Monte Carlo simulations had previously been used to determine the transition temperature to high precision, and a comparison at the transition temperature (see Fig. 12.5) showed quite clearly that a central peak was present in both simulation and experiment. The lack of the central peak in the mode coupling and renormalization group predictions must, therefore, be traced to inadequacies in the theory. The difference in the location of the spin wave peak in the spin dynamics simulations suggests that improvements in the model, e.g. by the inclusion of lattice vibrations, are needed if the agreement at T_N is to be quantitative. The estimate of the true, dynamic critical exponent z agreed with experiment but was slightly below theoretical predictions. A follow-up study (Tsai and Landau, 2003) examined finite size effects quite carefully and showed that both simulation and experiment were likely to have difficulty reaching the asymptotic regime of q-values.

Another success of the spin dynamics approach resulted from simulations of an anisotropic Heisenberg model designed to describe MnF_2 (Bunker and

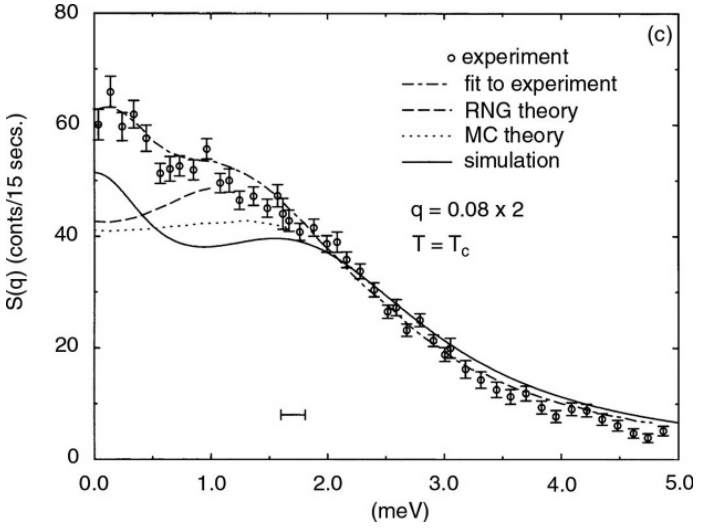

Fig. 12.5 Dynamic structure factor for $RbMnF_3$ as determined by experiment, theory, and simulation. Note that 'RNG theory' is renormalization group theory and 'MC theory' is mode coupling theory. After Tsai *et al.* (2000).

Landau, 2000). The simulations led to the prediction of a gap in the longitudinal spin wave frequency spectrum due to two-spin wave scattering, and this behavior was subsequently observed experimentally by polarized neutron scattering (Schweika *et al.*, 2002). Moreover, the impetus to perform the experiment actually came from the simulational results.

12.4 LANGEVIN EQUATIONS AND VARIATIONS (CELL DYNAMICS)

An alternative approach to the study of a system in the canonical ensemble is to allow the particles to undergo collisions with much lighter particles, the collection of which plays the role of a heat bath. In the same way, if a system has fluctuations on both very short and relatively long time scales, it is possible to use a rather large time step and allow the effect of rapid fluctuations to be described by a random noise plus a damping term. The relevant equations to be solved are then a set of Langevin equations:

$$m_i \ddot{\mathbf{r}}_i(t) = -\Gamma \dot{\mathbf{r}}_i(t) + \mathbf{F}_i(t) + \boldsymbol{\eta}(t), \tag{12.15}$$

where $\mathbf{F}_i(t)$ is the net force acting on the ith particle, Γ is the friction (damping) constant, and $\boldsymbol{\eta}(t)$ is a random, uncorrelated noise with zero mean. If the damping constant is chosen carefully the system will reach equilibrium and the resultant dynamic properties will not be affected by the choice of Γ. Such Langevin simulations were quite successful in the study of distortive phase transitions (Schneider and Stoll, 1978). In a different context, Grest and Kremer (1986) used Langevin dynamics methods to study polymers in a heat bath for different values of the friction. They found that this method not

only reproduced the Rouse model but remained effective at high densities and allowed differentiation between interchain couplings and the solvent.

When no acceleration is allowed to take place, the left-hand side of Eqn. (12.15) vanishes. The *Brownian dynamics* method solves the resultant equations, yielding a form of very 'overdamped' Langevin dynamics.

Langevin equations often result when one is not describing the system in full atomistic detail but rather on a more coarse-grained level, e.g. binary mixtures are described by a local concentration variable $c(\mathbf{r}, t)$, fluctuating in space ($\mathbf{r}$) and time (t). For a binary solid alloy as considered in Fig. 2.9, this variable $c(\mathbf{r}, t)$ arises by averaging over the concentrations of lattice sites contained in a cell of volume L^{d} (in d dimensions) centered at site $\mathbf{r}$. It is then possible to derive a non-linear differential equation for $c(\mathbf{r}, t)$, supplemented by a random force. The resulting Langevin equation is used to describe spinodal decomposition (see Chapter 2) and has been studied by simulations. An efficient discretized version of this approach is known as 'cell dynamics' technique (Oono and Puri, 1988).

12.5 MICROMAGNETICS

A method that is closely related to the Langevin approach has been used for many years in applied magnetism. The Landau–Lifshitz–Gilbert (LLG) equations of motion (Landau and Lifshitz, 1935; Gilbert, 1955) have been used for decades to determine the time dependence of the magnetization in diverse materials of practical importance to magnetic storage devices. In this approach (known as micromagnetics), however, the magnetization is a coarse-grained variable rather than the atomic spin vector and typically phenomenological values are taken for the effective damping coefficient. The time development of the magnetization $\mathbf{S}(\mathbf{x}, t)$ at position $\mathbf{x}$ and time t is given by the noisy form given in Eqn. (12.16) which can then be integrated in time

$$\frac{\partial \mathbf{S}(\mathbf{x}, t)}{\partial t} = \gamma \mathbf{S} \times \frac{\partial E(\{\mathbf{S}\})}{\partial \mathbf{S}(\mathbf{x})} + \alpha \gamma \hat{s} \times \left(\mathbf{S} \times \frac{\partial E(\{\mathbf{S}\})}{\partial \mathbf{S}(\mathbf{x})} \right) + \mathbf{S} \times \boldsymbol{\eta}(\mathbf{x}, t) \tag{12.16}$$

using numerical techniques ($\hat{s} = \mathbf{S}/S$). (In Eqn. (12.16) γ is the gyromagnetic ratio, α is the damping constant, $E\{S\}$ is the energy functional, and the final term represents the Gaussian distributed random noise.) The results can then be compared with experiment. Unfortunately, it is often quite difficult to determine what the parameters should be from a fundamental starting point, and the results are often in disagreement with experiment. In an effort to lessen the gap between experiment and simulation Grinstein and Koch (2003) recently showed how a temperature dependent renormalization group theory could be used to determine the effective exchange coefficient in the equations. The implementation of this approach to permalloy (a favorite, important material

for the testing of methods in applied magnetism) showed a dramatic decrease in the predicted critical temperature to a value that is roughly correct.

12.6 DISSIPATIVE PARTICLE DYNAMICS (DPD)

In the context of simulating soft matter systems over mesoscopic (rather than truly atomistic) scales of space and time, the idea of coarse-graining the system so that groups of atoms are treated together as one effective 'particle' is attractive. Unlike the 'united atom' approach familiar from polymer simulations in which one replaces several atoms, e.g. a CH_2 group in an alkane chain, by one 'united atom' but otherwise aims at a chemically realistic description of the system, here the effective particle represents many atoms and no attempt is made to provide a realistic description of particular materials. Rather, generic features are to be elucidated qualitatively, and therefore one chooses potentials between effective particles that are computationally convenient. Thus, forces between particles are taken to be pair-wise and decrease linearly with distance, r, from a finite maximum value of $r = 0$ up to maximum distance $r = r_c$, and the force is zero for all $r \geq r_c$. Using Newton's equations of motion, i.e. carrying out molecular dynamics (MD) simulations, such a choice allows much larger time steps than are normally possible. Consequently, one may proceed to much longer times.

As the name of the method already indicates, one includes not only the conservative forces as described above but also a random force and friction forces (the latter two being related by a fluctuation-dissipation relation). However, the method fundamentally differs from the standard Brownian dynamics method where one simulates a Langevin equation (see Section 12.4), because the friction force is not simply proportional to the velocity, $\mathbf{v}$, of an effective particle. Instead it is proportional to the relative velocity $\mathbf{v}_{ij} = \mathbf{v}_j - \mathbf{v}_i$, between a pair of particles – as a result, both the friction force and the random forces are also pair-wise forces. A standard choice for the random force is (Groot, 2004) $\mathbf{F}_{ij}^R = \sigma\omega(r_{ij})\hat{r}_{ij}z/\sqrt{\delta t}$, where α characterizes the strength of the random force, $\omega(r) = 1 - r$ for $r < 1$ and zero else, z is a random variable with zero mean and unit variance, $\hat{r}_{ij}$ is a unit vector along $\mathbf{r}_{ij} = \mathbf{r}_j - \mathbf{r}_i$, and δt the time step of the MD integration. The friction (or drag) force is then

$$\mathbf{F}_{ij}^D = -\frac{1}{2k_B T}[\sigma\omega(r_{ij})]^2 \hat{r}_{ij}(\mathbf{v}_{ij} \cdot \mathbf{r}_{ij}). \tag{12.17}$$

This DPD method can be shown to yield a Boltzmann distribution in equilibrium corresponding to the NVT ensemble, but at the same time it leads to the correct description of hydrodynamics (Espanol, 1995; Espanol and Warren, 1995; Groot and Warren, 1997). This statement would be true for neither the Brownian dynamics method (momentum transport is not described correctly) nor the 'thermostat' used in the context of MD simulations to realize the NVT ensemble rather than the NVE ensemble. Consequently, the DPD random

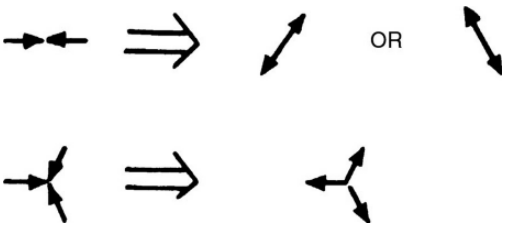

Fig. 12.6 Lattice gas cellular automata collision rules for particle movement on a triangular lattice.

and friction forces are now becoming increasingly popular as a 'thermostat' in standard MD simulations (using more realistic inter-particle forces, rather than the coarse-grained linear variation mentioned above).

Although the DPD approach has been proposed only rather recently (Hoogerbrugge and Koelman, 1992), its applications are already rather widespread (e.g. structure formation of block copolymer mesophases, including effects of shear flow, surfactant solutions, biomembrane deformation and rupture, etc.). A review of this method and related methods can be found in Karttunen *et al*. (2004).

12.7 LATTICE GAS CELLULAR AUTOMATA

An inventive approach to the use of cellular automata to study fluid flow (Frisch *et al*., 1986) incorporates the use of point masses on a regular lattice for simulations in which space, time, and velocity are discretized. In two dimensions, particles move on a triangular lattice, and particle number and momentum are conserved when they collide. Each particle has a vector associated with it which points along one of the lattice directions. On the triangular lattice each point has six nearest neighbors, and thus only six different values of velocity are allowed. The system progresses in time as a cellular automaton in which each particle may move one nearest neighbor distance in one time step. The system is updated by allowing particles which collide to scatter according to Newton's laws, i.e. obeying conservation of momentum. Examples of collision rules are shown schematically in Fig. 12.6. This 'lattice gas cellular automata' approach to fluid flow has been shown, at least in the limit of low velocity, to be equivalent to a discrete form of the Navier–Stokes equation, and represents a potentially very fast method to study fluid flow from a microscopic perspective. In the case of collisions which involve non-zero momentum this procedure is always used. If the total momentum of colliding particles is zero, there is a degeneracy in the resulting outcome (see Fig. 12.6) and the choice can be made by a predetermined 'tie-breaker' or through the use of a random number generator. Lattice gas models have now been used extensively to examine a number of different physical situations including flow in complex geometries, phase separation, interface properties, etc. As a demonstration of the nature of the results that one may obtain, we show in Fig. 12.7 a typical flow pattern obtained when a flat plate is inserted in front of the moving fluid.

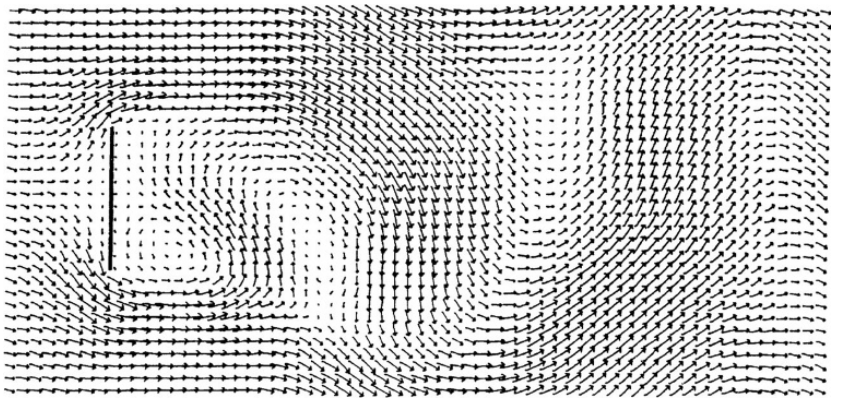

Fig. 12.7 Two-dimensional flow past a flat plate (flow from left to right) as obtained from a cellular automata lattice gas simulation. From d'Humieres *et al.* (1985).

A more complete description of lattice gas cellular automata, as well as more extensive sample results, can be found elsewhere (Rothman and Zaleski, 1994).

12.8 LATTICE BOLTZMANN EQUATION

A development that has already found extensive application in problems of fluid dynamics, complex fluids, polymers, etc., is the lattice Boltzmann equation approach. An outgrowth of lattice gas cellular automata the method replaces the Boolean variables n_i at each site i, as described in the previous section, with the corresponding ensemble-averaged populations $f_i = \langle n_i \rangle$.

Noise problems are thereby circumvented because the f_i are themselves averaged quantities, but the limitation is the loss of information about correlations. The details of specific applications turn out to be quite important and are beyond the scope of the present treatment. For more complete descriptions see Succi (2001) and Kendon *et al.* (2001).

In a fascinating recent study, Horbach and Succi (2006) compared results of simulated fluid flow in a simple dense liquid, passing an obstacle in a two-dimensional thin film geometry obtained using molecular dynamics, with those from lattice Boltzmann simulations. By the appropriate mapping of length and time units from lattice Boltzmann to molecular dynamics, the velocity field, shown in Fig. 12.8, as obtained from molecular dynamics, is quantitatively reproduced by lattice Boltzmann.

12.9 MULTISCALE SIMULATION

For many problems in materials science and biological soft matter, non-trivial structures occur over many length scales: chemical details on the scale of 1 Å may be simultaneously important for non-trivial ordering phenomena on the nanoscopic and mesoscopic scales. In principle one would like to deal with systems of the linear dimension of a micrometer or larger, i.e. one would have to deal with systems comprising billions of atoms. Sometimes there may be a

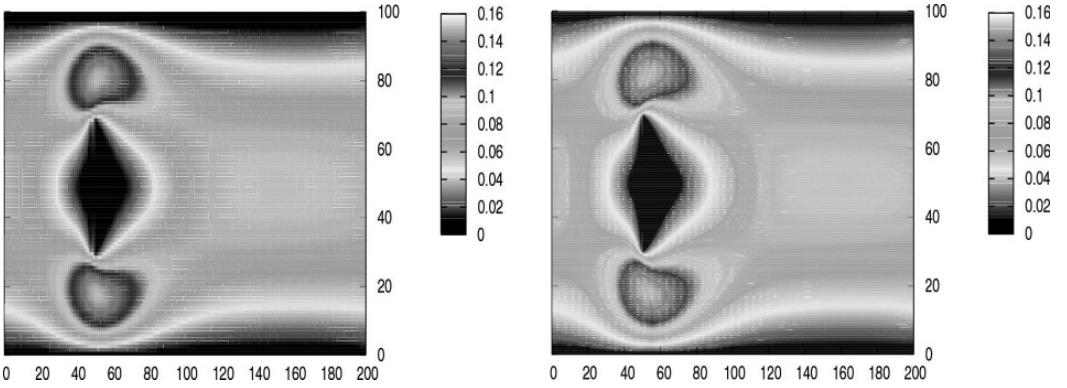

Fig. 12.8 Flow past a rigid obstacle. (a) The flow map shows the magnitude of the velocity field at steady state as obtained from a molecular dynamics simulation. (b) The same result as obtained from a lattice Boltzmann simulation. From Horbach and Succi (2006).

similar spread of time scales; e.g. in a glass-forming polymer melt the spectrum of relaxation times extends from picoseconds to macroscopic times.

Of course, there is no general solution to the challenge of mastering such widely varying scales of length and time (Brandt *et al.*, 2001); however, there are special cases where progress can be made by combining different types of simulation algorithms that are suitable for different scales to treat a single large-scale problem. Such an approach is termed 'multiscale simulation'. Such a special case may occur when great atomistic detail is required only in a small region of a large-scale system. Consider, e.g., the problem of crack propagation in a crystal (Fig. 12.2): the most important regions are in the immediate neighborhood of the crack tip; however, some elastic distortions due to the strain fields that are generated are felt quite far away from the crack. For this problem, Abraham (2000) describes a newly proposed multiscale simulation approach as follows: in the immediate environment of the crack tip(s) (i.e. a region of the order of 10^2 atoms) *ab initio* molecular dynamics (Car and Parrinello, 1985) is used. Hence electronic structure calculations enter the energetics in this highly non-linear and deformed region of the crystal. Outside this 'core' a much larger region ($\sim 10^6$ atoms) is treated by classical MD methods, while elastic deformations yet farther away from the crack tip(s) are described using a numerical implementation of the continuum theory of elasticity (i.e. the 'finite element method' (FEM)). Of course, the key challenge of such an approach is to identify a robust 'handshaking' method to 'glue together' these complementary techniques so that the results fit together in the transition zones where one method gives way to the next one. This was done by defining overlap regions where two methods were applied together, e.g., the atoms in the outer zone of the Car–Parrinello region around the crack tip were also part of the region treated by classical MD. A constraint was then enforced that the positions of the same atoms were identical using both methods. For details about how such a 'handshaking' between methods can be implemented we refer the reader to the original literature.

Still different types of approaches are needed for simulations of polymeric materials (Paul *et al.*, 1991; Tschöp *et al.*, 1998; Baschnagel *et al.*, 2000; Girard and Müller-Plathe, 2004). In amorphous (fluid or solid) polymers a chemically realistic, atomic level description (based on torsional and bond angle potentials derived from quantum chemistry, etc.) is indispensable to account for the physical properties on the macroscale. At the same time, however, the large macromolecules form (interpenetrating) random walk-like coils, and mesoscopic structures may occur if block-copolymers or liquid crystalline polymers are involved that may form ordered superstructures. The approach attempted in the literature so far is to try a 'mapping' from the chemically realistic scale to simplified models (e.g. lattice models like the bond fluctuation model of polymers, see Section 4.7.3, or bead-spring type models) using a coarse-graining procedure. One approach is to use each effective bond of the coarse-grained model to represent a whole group of subsequent 'chemical monomers' along the backbone of the chain. All the parameters of this coarse-grained model (including the effective potentials for the length and bond angles of the effective bonds, etc.) have to be derived systematically from MD simulation of the chemically realistic model. Using this information, the large-scale structure of the polymers in the framework of the coarse-grained model can then be equilibrated by standard MC or MD methods. If the goal is to consider properties that depend on chemical detail, however, the effective bonds then need to be replaced by the corresponding 'chemical monomers' and re-equilibrated again ('reverse mapping', see, e.g. Girard and Müller-Plathe (2004)). All of these methods are still under development at the time of writing, and hence we refrain from providing any details.

For problems such as the long range order of block copolymer mesophases, systems containing many thousands of polymer chains would be desirable. Murat and Kremer (1998) suggested mapping a polymer chain onto a soft ellipsoid, and they derived the parameters for such a model from the bead-spring chain model. However, we are not aware that the full gap from quantum chemistry to mesophase structures has been bridged.

Many molecules of pharmacological importance are not only complex, but also function by bonding covalently to their targets. In order to simulate such systems it becomes important to include quantum mechanics, and important steps have been taken by combining Car–Parrinello quantum mechanics with molecular mechanics (QM/MM method). In this approach a system is partitioned into a region that is treated quantum mechanically and a region that is treated with a molecular mechanics force field. For an overview of this approach, see Rothlisberger and Carloni (2006).

12.10 MULTIPARTICLE COLLISION DYNAMICS

There are many research efforts on soft matter (including problems inspired by biology and medicine) where mesoscopic particles are transported by a fluid medium within a confined geometry (e.g. transport of red blood cells in

the human body, flow of colloidal particles in a microfluidic device, etc.). In such circumstances, the basic length scale of interest is that of the transported particle, while spatial correlations on the scale of the molecules of the fluid in which these particles move do not matter at all. However, these fluid particles must not be neglected completely: they transmit the long-range hydrodynamic interaction that is inversely proportional to the fluid viscosity. Note that the effect of the fluid on the motion of such a Brownian particle cannot simply be absorbed in the time scale of a Langevin equation description (remember the discussion in Section 12.4). For example, if we describe the effect of the solvent fluid on the diffusion of a long macromolecule (of chain length N) simply in terms of random, delta-correlated forces (as assumed in Eqn. (12.15)), we obtain a diffusion constant for the polymer that is inversely proportional to its chain length N (the 'Rouse model' of polymer dynamics, see Section 6.6.3). However, in reality due to hydrodynamic correlations the polymer diffuses much faster, with a diffusion constant (Stokes law) that is inversely proportional to the product of solvent viscosity and the radius R of the polymer coil. The latter scales as $R \propto N^{3/5}$ in good solvents, or as $R \propto N^{1/3}$ in poor solvents, where the coil is collapsed into a dense globule. Thus, taking hydrodynamics into account may speed up the motions by many orders of magnitude in comparison with the simple Langevin dynamics description of Section 12.4. Of course, when we have different species in a dispersion, e.g. a mixture of polymers and spherical (or rod-like) colloidal particles, this speed-up cannot be accounted for by uniform adjustment of the time scale.

In principle this hydrodynamic interaction between particles of mesoscopic size can be described by numerical methods of fluid dynamics, such as the lattice Boltzmann method (Section 12.8). However, in situations of geometrical confinement, such as flow in blood vessels or microfluidic devices, the hydrodynamic boundary conditions at the confining walls (stick versus slip boundary conditions) are somewhat cumbersome to take care of.

A useful approach to such problems is the multiparticle collision dynamics (MPC) method (Malevanets and Kapral, 1999, 2000). Here the solvent is represented by point-like non-interacting particles (of mass m each) that exchange momentum with the mesocopic particles (colloids or bacteria or cells, etc.) through collision steps. Local conservation of momentum and mass of all particles is a crucial ingredient to obtaining a simulation compatible with hydrodynamics. In between these collision steps, the configurations of all particles evolve according to ordinary molecular dynamics methods (e.g. using the velocity Verlet algorithm described in Section 12.2.). In order to carry out the collision step, one divides the system into cells which are chosen such that each cell can contain at most a single mesoscopic particle cell but must contain a large number of fluid particles (e.g. at least 10 such particles). In the collision step, the velocities of all particles in each cell are updated by a rotation of their relative velocities, $\mathbf{v}_i = \mathbf{u} + \underline{R}(\alpha) \cdot \delta\mathbf{v}_i$, where $\mathbf{u}$ is the mean velocity in the cell, $\delta\mathbf{v}_i = \mathbf{v}_i - \mathbf{u}$, $\mathbf{v}_i$ being the velocity of the ith particle, and $\underline{R}(\alpha)$ is a rotation matrix with angle α around a randomly chosen rotation axis. (This algorithm is also called the 'stochastic rotation algorithm'.) Note that in the

'streaming step' in between collisions the solvent particles evolve according to free flight in the absence of uniform external forces. Of course, one may wish to allow the mesoscopic particles also to interact with some potential, and the effect of the forces then acting on them is taken care of through the molecular dynamics algorithm, as has already been mentioned above.

From this description it is evident that hydrodynamics is only described on length scales larger than the chosen cell size, which is comparable to the size of the mesoscopic particles. In a real system, hydrodynamics may already hold on much smaller scales (distances of a few solvent molecules diameters), but for most cases of interest such small-scale phenomena are quite unimportant. The choice of parameters for this algorithm is not unique but can be varied over a wide range in order to adapt the algorithm to the problem at hand (e.g. the solvent viscosity can be varied over a large range). Also, different thermostats can be combined with this algorithm, but such technical details are beyond the scope of consideration here. It is, however, worthwhile mentioning the implementation of boundary conditions at walls: 'perfect slip' is realized by specular reflection of particles, while 'perfect stick' is realized by the 'bounce back' rule (Whitmer and Luijten, 2010).

This method has recently found very widespread use (see Gompper *et al.* (2009) for an early review). As a typical example, we mention the study of spinodal decomposition in thin films of colloid-polymer mixtures following sudden compression of the system. Typical linear dimensions used in such a simulation were $256 \times 256 \times 10$, using the colloid diameter as the unit of length (with the polymers having a diameter of 0.8). A typical simulation then needed to use 236 859 colloids, 1 019 022 polymers, and 52 million solvent particles. Since the slow formation of large-scale domain structures required running the system for more than 10^4 molecular-dynamics time units, it is clear that such studies of multiscale problems can only be performed by well-optimized codes on massively parallel multiprocessor machines. By such efforts, Winkler *et al.* (2013) could clarify the effect of hydrodynamic interactions on late-stage domain growth for spinodal decomposition in confined geometry.

REFERENCES

Abraham, F. F. (1996), *Phys. Rev. Lett.* **77**, 869.

Abraham, F. F. (2000), *Int. J. Mod. Phys. C* **11**, 1135.

Alder, B. J. and Wainwright, T. E. (1970), *Phys. Rev. A* **1**, 18.

Allen, M. P. and Tildesley, D. J. (1987), *Computer Simulations of Liquids* (Clarendon Press, Oxford).

Andersen, H. C. (1980), *J. Chem. Phys.* **72**, 2384.

Baschnagel, J., Binder, K., Doruker, P., Gusev, A. A., Hahn, O., Kremer, K., Mattice, W. L., Müller-Plathe, F., Murat, M., Paul, W., Santos, S., Suter, U. W., and Tries, V. (2000), *Adv. Polymer Sci.* **152**, 41.

Beazley, D. M. and Lomdahl, F. S. (1994), *Parallel Computing* **20**, 173.

Berendsen, H. J. C. and Van Gunsteren, W. F. (1986), in *Molecular Dynamics Simulation of Statistical Mechanical*

Systems, Proceedings of the Enrico Fermi Summer School, Varenna (Soc. Italiana di Fisica, Bologna).
Brandt, A., Bernholc, J., and Binder, K. (eds.) (2001), *Multiscale Simulations in Physics and Chemistry* (IOS Press, Amsterdam).
Bunker, A. and Landau, D. P. (2000), *Phys. Rev. Lett*. **85**, 2601.
Burden, R. L., Faires, J. D., and Reynolds, A. C. (1981), *Numerical Analysis* (Prindle, Weber, and Schmidt, Boston).
Car, R. and Parrinello, M. (1985), *Phys. Rev. Lett*. **55**, 2471.
Chen, K. and Landau, D. P. (1994), *Phys. Rev. B* **49**, 3266.
d'Humières, D., Pomeau, Y., and Lallemand, P. (1985), *C. R. Acad. Sci. II* **301**, 1391.
Duane, S., Kennedy, A. D., Pendleton, B. J., and Roweth, D. (1987), *Phys. Lett. B* **195**, 216.
Espanol, P. (1995), *Phys. Rev. E* **52**, 1736.
Espanol, P. and Warren, P. (1995), *Europhys. Lett*. **19**, 155.
Evans, D. J. and Morriss, G. P. (1984), *Comput. Phys. Rep*. **1**, 297.
Evans, D. J. and Morriss, G. P. (1990), *Statistical Mechanics of Nonequilibrium Liquids* (Academic, London).
Evertz, H. G. and Landau, D. P. (1996), *Phys. Re v. B* **54**, 12302.
Frisch, U., Hasslacher, B., and Pomeau, Y. (1986), *Phys. Rev. Lett*. **56**, 1505.
Gerling, R. W. and Landau, D. P. (1984), *J. Magn. Mag. Mat*. **45**, 267.
Gilbert, T. L. (1955), *Phys. Rev*. **100**, 1243.
Girard, S. and Müller-Plathe, F. (2004), in *Novel Methods in Soft Matter Simulations*, eds. M. Karttunen, I. Vattulainen, and A. Lukkarinen (Springer, Berlin), p. 327.
Gompper, G., Ihle, T., Kroll, D. M., and Winkler, R. G. (2009), *Adv. Polym. Sci.* **221**, 1.
Grest, G. S. and Kremer, K. (1986), *Phys. Rev. A* **33**, 3628.
Grinstein, G. and Koch, R. H. (2003), *Phys. Rev. Lett*. **90**, 207201.
Groot, R. D. (2004), in *Novel Methods in Soft Matter Simulations*, eds. M. Karttunen, I. Vattulainen, and A. Lukkarinen (Springer, Berlin), p. 5.
Groot, R. D. and Warren, P. (1997), *J. Chem. Phys*. **107**, 4423.
Hoogerbrugge, P. J. and Koelman, J. M. V. A. (1992), *Europhy. Lett*. **19**, 155.
Hoover, W. G. (1985), *Phys. Rev. A* **31**, 1695.
Horbach, J. and Succi, S. (2006), *Phys. Rev. Lett*. **96**, 224 503.
Kadau, K., Germann, T. C., and Lomdahl, P. S. (2004), *Int. J. Mod. Phys. C* **15**, 193.
Karttunen, M., Vattulainen, D., and Lukkarinen, A. (eds.) (2004), *Novel Methods in Soft Matter Simulations* (Springer, Berlin).
Kendon, V. M., Cates, M. E., Pagonabarraga, I., Desplat, J. C., and Bladon, P. (2001), *J. Fluid Mech*. **440**, 147.
Krech, M., Bunker, A., and Landau, D. P. (1998), *Comput. Phys. Commun*. **111**, 1.
Laio, A. and Parrinello, M. (2002), *Proc. Natl Acad. Sci. USA* **99**, 12, 562.
Laio, A. and Parrinello, M. (2006), in *Computer Simulations in Condensed Matter: From Materials to Chemical Biology*, eds. M. Ferrario, G. Ciccotti, and K. Binder (Springer, Heidelberg), vol. 1, p. 315.
Landau, L. D. and Lifshitz, E. M. (1935), *Phys. Z. Sowjetunion* **8**, 153.
Malevanets, A. and Kapral, R. (1999), *J. Chem. Phys*. **110**, 8605.
Malevanets, A. and Kapral, R. (2000), *J. Chem. Phys*. **112**, 7260.
Murat, M. and Kremer, K. (1998), *J. Chem. Phys*. **108**, 4340.
Nelson, D. R. and Fisher, D. S. (1977), *Phys. Rev. B* **16**, 4945.
Nosé, S. (1984), *Mol. Phys*. **52**, 255.
Oono, Y. and Puri, S. (1988), *Phys. Rev. A* **38**, 434.

Parrinello, M. (1997), *Solid State Commun*. **102**, 107.
Pastorino, C., Kreer, T., Müller, M., and Binder, K. (2007), *Phys. Rev. E* **76**, 026 706.
Paul, W., Binder, K., Kremer, K., and Heermann, D. W. (1991), *Macromolecules* **24**, 6332.
Rapaport, D. C. (1988), *Phys. Rev. Lett*. **60**, 2480.
Rapaport, D. C. (1995), *The Art of Molecular Dynamics Simulation* (Cambridge University Press).
Roth, J., Gähler, F., and Trebin, H.-R. (2000), *Int. J. Mod. Phys. C* **11**, 317.
Rothlisberger, U. and Carloni, P. (2006) in *Computer Simulations in Condensed Matter: From Materials to Chemical Biology*, eds. M. Ferrario, G. Ciccotti, and K. Binder (Springer, Heidelberg), vol. 2, p. 449.
Rothman, D. H. and Zaleski, S. (1994), *Rev. Mod. Phys*. **66**, 1417.
Schneider, T. and Stoll, E. (1978), *Phys. Rev*. **17**, 1302.
Schweika, W., Maleyev, S. V., Brückel, T., Plakhty, V. P., and Regnault, L.-P. (2002), *Europhys. Lett*. **69**, 446.
Succi, S. (2001), *The Lattice Boltzmann Equation* (Clarendon Press, Oxford).
Tavazza, F., Nurminen, L., Landau, D. P., Kuronen, A., and Kaski, K. (2004), *Phys. Rev. B* **70**, 184103.
Tsai, S.-H. and Landau, D. P. (2003), *Phys. Rev. B* **67**, 104411.
Tsai, S.-H., Bunker, A., and Landau, D. P. (2000), *Phys. Rev. B* **61**, 333.
Tschöp, W., Kremer, K., Batoulis, J., Bürger, T., and Hahn, O. (1998), *Acta Polymer* **49**, 61, 75.
Tuckerman, M., Martyna, G. J., and Berne, B. J. (1992), *J. Chem. Phys*. **97**, 1990.
Verlet, L. (1967), *Phys. Rev*. **159**, 98.
Verlet, L. (1968), *Phys. Rev*. **165**, 201.
Villain, J. (1974), *J. Phys. (Paris)* **35**, 27.
Voter, A. F. (1997), *Phys. Rev. Lett*. **78**, 3908.
Whitmer, J. K. and Luijten, E. (2010), *J. Phys.: Condens. Matter* **22**, 104106.
Winkler, A., Virnau, P., Binder, K., Winkler, R. G., and Gompper, G. (2013), *J.* Chem. Phys. **138**, 054901.